HHS Public Access

Author manuscript

Stem Cells. Author manuscript; available in PMC 2020 February 01.

Published in final edited form as:

Stem Cells. 2019 February ; 37(2): 202–215. doi:10.1002/stem.2941.

GLIS3 Transcriptionally Activates WNT Genes to Promote Differentiation of Human Embryonic Stem Cells into Posterior Neural Progenitors

Kilsoo Jeon[1], **Dhirendra Kumar**[2], **Amanda E. Conway**[2], **Kyeyoon Park**[3], **Raja Jothi**[2], and **Anton M. Jetten**[1,*]

[1]Immunity, Inflammation and Disease Laboratory, National Institute of Environmental Health Sciences, National Institutes of Health, Research Triangle Park, NC 27709

[2]Epigenetics & Stem Cell Biology Laboratory, National Institute of Environmental Health Sciences, National Institutes of Health, Research Triangle Park, NC 27709

[3]NIH Stem Cell Unit, National Institute of Neurological Disorders and Stroke, National Institutes of Health, Bethesda, MD 20814

Abstract

Anterior-posterior (A-P) specification of the neural tube involves initial acquisition of anterior fate followed by the induction of posterior characteristics in the primitive anterior neuroectoderm. Several morphogens have been implicated in the regulation of A-P neural patterning; however, our understanding of the upstream regulators of these morphogens remains incomplete. Here, we show that the Krüppel-like zinc finger transcription factor GLI-Similar 3 (GLIS3) can direct differentiation of human embryonic stem cells (hESCs) into posterior neural progenitor cells (NPCs) in lieu of the default anterior pathway. Transcriptomic analyses reveal that this switch in cell fate is due to rapid activation of WNT signaling pathway. Mechanistically, through genome-wide RNA-Seq, ChIP-Seq and functional analyses, we show that GLIS3 binds to and directly regulates the transcription of several WNT genes, including the strong posteriorizing factor WNT3A, and that inhibition of WNT signaling is sufficient to abrogate GLIS3-induced posterior specification. Our findings suggest a potential role for GLIS3 in the regulation of A-P specification through direct transcriptional activation of WNT genes.

Graphical Abstract

*To whom correspondence should be addressed, Tel: 919-541-2768; Fax: 919-541-4133, jetten@niehs.nih.gov.

AUTHOR CONTRIBUTIONS

KJ and AMJ designed experiments; KJ conducted all the experiments; AEC conducted ChIP-Seq studies; DK performed all the bioinformatics analyses; KJ, DK, KP, RJ, and AMJ analyzed data; KJ, RJ, and AMJ wrote the manuscript.

Supporting INFORMATION

Paper contains an additional 7 Supporting Figures and Figure legends, and 7 Supporting Tables.

Accession number

RNA-Seq and ChIP-Seq data generated for this study have been deposited in the GEO repository under the accession number GSE109562.

DECLARATION OF INTERESTS: A.M.J declare stock ownership in WLL, SENS, and VNTV. All other authors have declared no conflict of interest.

Expression of the Krüppel-like zinc finger transcription factor GLIS3 in human embryonic stem cells induces differentiation along the posterior neural progenitor lineage instead of the default anterior lineage through the transcriptional activation of the strong posteriorizing factor WNT3A.

Keywords

GLIS3; human embryonic stem cells; WNT signaling; gene transcription; neural progenitors; anterior-posterior patterning

INTRODUCTION

WNT ligands are secreted glycoproteins, which play critical roles in the regulation of many stages of embryonic development [1–4]. Binding of WNTs to seven-transmembrane-domain Frizzled receptors causes activation of Dishevelled (DSH), a family of proteins involved in the activation of canonical and noncanonical WNT signaling pathways. Activation of the canonical WNT pathway results in the accumulation and nuclear translocation of β-catenin, which upon interaction with lymphoid enhancer-binding factor (LEF1 or TCF1α) activates transcription. WNT ligands are expressed early in the developing nervous system and have been implicated in many aspects of neural development, including the regulation of cell proliferation, neural cell fate determination, synapse formation, and axon growth [4–10]. Abnormalities in WNT signaling result in aberrant neural development and have been implicated in several human pathologies [5, 8].

Early during development, the neural tube is subdivided into several regions along the anterior-posterior (A-P) axis that will form the forebrain, midbrain, hindbrain and spinal cord. The importance of WNT signaling in the regulation of a A-P neural patterning has been well-established. In WNT3A-deficient embryos, midbrain, hindbrain and spinal cord are poorly developed and is associated with expression of forebrain marker genes, including *OTX2* and *PAX6*, whereas expression of the homeobox gene, *GBX2*, which is required for hindbrain development, is repressed [3, 9–16]. Subsequent studies on the differentiation of human embryonic stem cells (hESCs) into neural progenitor cells (NPCs) demonstrated that hESCs by default differentiate along the anterior NPC lineage and can posteriorize under the influence of various caudalizing signals [17–22]. Morphogens, like retinoic acid and fibroblast growth factors (FGFs), promote specification of posterior NPC differentiation. Although WNT proteins, particularly WNT3A, act as strong posteriorizing factors and function as critical regulators of the regional identity along the A-P axis during early neural development [4, 8–10, 16, 21, 23, 24], our understanding of the regulation of WNT gene expression remains incomplete.

GLI Similar 3 (GLIS3), a Krüppel-like zinc finger transcription factor, plays a critical role in the regulation of many biological processes, including pancreatic beta cell generation, spermatogenesis, and thyroid hormone biosynthesis [25–31]. Recently, GLIS3 was shown to effectively promote reprogramming of somatic cells into embryonic stem cells [32, 33]. GLIS3 is expressed in a spatiotemporal manner during early embryonic neural development suggesting a potential regulatory function [25]. A role for GLIS3 in the nervous system is further supported by studies showing that GLIS3-deficiency leads to the development of

mild mental retardation and facial dysmorphism, and the association of single nucleotide polymorphisms (SNPs) in *GLIS3* with an increased risk of Parkinson's and Alzheimer's disease [34–38]. A recent study found a correlation between *Glis3* variants and a significant reduction in dendritic complexity and spine density, important characteristics in several neurodegenerative diseases [39]. Overexpression of GLIS3 was reported to be associated with ependymomas, tumors arising from the ependyma of the central nervous system [40]. Collectively, these studies suggest that GLIS3 has multiple regulatory functions in the neural system.

Here, we show that GLIS3 expression promotes posterior specification of hESC-derived NPCs, in lieu of the default anterior NPC fate, through its activation of WNT signaling. Mechanistically, we show that GLIS3 binds to and transcriptionally activates several WNT genes, including *WNT3A* encoding a strong posteriorizing factor. Inhibition of WNT signaling is sufficient to abrogate GLIS3-induced posterior specification. Altogether, our study identifies GLIS3 as an upstream transcriptional activator of WNT gene expression and through this activation induces posterior specification of NPCs.

MATERIALS AND METHODS

Human ES cell culture

H9 and H1 human embryonic stem cells (hESC; NIH code: WA09 and WA01, respectively) were initially grown on mitotically inactivated primary mouse embryonic fibroblasts (MEF) in KnockOut DMEM/F12 supplemented with 20% KnockOut serum replacement (KSR), 0.1 mM β-mercaptoethanol, and non-essential amino acids (Gibco). Adaptation to single-cell based non-colony type monolayer culture of hESC was carried out as previously described [41–43]. Briefly, the cell pellets of hESC were dissociated with 1× Accutase (Innovative Cell Technologies) for 15 min and subsequently resuspended in mTeSR1 defined medium (Stemcell Technologies), and centrifuged at 2000 rpm for 5 min. Dissociated single cells were then plated at a density of 2×10^6 cells in 6-well dishes coated with 2.5% hESC-qualified Matrigel (Corning) in mTeSR1 containing 10 μM ROCK inhibitor (Tocris Bioscience). After 24 h, the ROCK inhibitor was withdrawn and hESC were allowed to grow as a monolayer. hESC were passaged every 4–5 days, replated at a dilution of 1:6 and maintained in mTeSR1 in Matrigel-coated culture dishes.

Generation of doxycycline (DOX)-inducible Flag-GLIS3-HA hESCs

pIND20(Flag-GLIS3-HA) was generated by recombination of Flag-GLIS3-HA into the DOX-inducible lentiviral vector pIND20 [44]. Lentivirus was generated by transient transfection of pIND20(Flag-GLIS3-HA) in HEK293T cells. H9 hESCs grown in mTeSR1 were infected overnight with pIND20(Flag-GLIS3-HA) lentivirus and then selected in medium supplemented with 50 μg/ml G418 (Invitrogen). The DOX-inducible Flag-GLIS3-HA H9 hESCs are referred to as G3-hESCs. Flag-GLIS3-HA expression was induced by the addition of 100 μg/ml DOX (Sigma-Aldrich). Stably expressing pIND20-Flag-GLIS3-HA cell lines were also established from H1 hESCs and HEK293T cells and are referred to as G3-H1-hESCs and G3-HEK293T, respectively.

Induction of neural progenitor cells

hESC cultured in mTeSR1 were dissociated with Accutase for 5 min, resuspended, and plated in Matrigel-coated dishes at a density of 2×10^5 cells in presence of ROCK inhibitor. The next day, the culture medium was switched to neural induction medium (DMEM without vitamin A plus 1% B27 (Gibco)) supplemented with 1 μM dorsomorphin and 5 μM SB431542 (Tocris Bioscience), inhibitors of the activin/TGFβ/BMP pathways. The medium was subsequently changed every other day. At day 7, NPCs were dissociated with Accutase, replated, and maintained in STEMdiff neural progenitor cell (NPC) medium (Stemcell Technologies) in Matrigel-coated dishes.

Quantitative PCR (qRT-PCR)

Total RNA was isolated using the PureLink RNA Mini Kit (Invitrogen) according to the manufacturer's protocol and cDNA generated using a High Capacity cDNA Reverse Transcription kit (Applied Biosystems). qRT-PCR was carried out using SYBER Green Supermix (Bio-Rad). Primer sequences are listed in Supporting Information Table S1. The deltadeltaCT method [45] was used to determine the relative fold change in the expression of each specific gene using the housekeeping gene GAPDH as the normalizer. All data were derived from biological triplicates.

Immunocytochemical staining

Cells were fixed in 4% paraformaldehyde at room temperature (RT) for 15 min, washed twice with Dulbecco's phosphate-buffered saline (DPBS), and then permeabilized with 0.2% Triton X-100 for 20 min at RT. Cells were then washed twice with DPBS and blocked in DPBS containing 5% normal goat or donkey serum for 1 h. Cells were incubated overnight at 4°C in blocking buffer with the primary antibody indicated, washed twice with DPBS, and subsequently incubated for 1 h at RT with secondary antibodies and washed twice with DPBS. Antibodies are listed in Supporting Information Table S2. Nuclei were identified by 4', 6'-diamidino-2-phenylindole (DAPI). Fluorescence was observed with a Zeiss LSM-710 confocal microscope.

Flow cytometry

For flow cytometry (FACS) analysis, single cell suspensions were obtained by dissociating cells using Accutase for 10 min at 37°C. Cells were then washed twice with FACS buffer (PBS, 1% BSA) and fixed with 4% paraformaldehyde (PFA), permeabilized with 0.2% Triton X-100, and resuspended at 10^6 cells/100 μl. Cells were stained for 1 h on ice with the antibodies indicated, washed, and resuspended in FACS buffer. FACS analysis was performed using a FACScan flow cytometer and Cell Quest software.

Reporter assays

The luciferase reporter construct pGL4.10-WNT3A-Luc was generated by cloning the −1690 to +317 upstream regulatory region of *WNT3A* into the *Eco*RV/*Hind*III sites of pGL4.10. HEK293 cells were transfected with the pGL4-WNT3A-Luc and pCMV-β-Gal reporter plasmids and pGL4-empty or the expression vector p3×Flag-CMV-GLIS3 encoding full-length GLIS3 in Opti-MEM using lipofectamine 2000 (Invitrogen). Similarly, hESC-

pIND20(Flag-GLIS3-HA) were seeded in Matrigel-coated 12-well dishes at a density of 10^6 cells/well in mTeSR1 with 10 μM ROCK inhibitor. After 24 h, cells were transfected with pGL4-WNT3A-Luc and pCMV-β-Gal in Opti-MEM using Lipofectamine 2000 and 24 h later treated with DOX to induce Flag-GLIS3-HA. Cells were harvested after 24 h by scraping them directly into 125 μl reporter lysis buffer. Luciferase activity and β-galactosidase levels were measured using a luciferase assay kit (Promega) and a luminometric β-galactosidase detection kit (Clontech) following the manufacturer's protocol. Experiments were carried out in triplicate.

Western blot analysis

For Western blotting, cells were washed three times in cold PBS and then scraped into lysis buffer. After a 30 min incubation on ice, lysates were centrifuged and protein in the supernatants quantified using the Pierce BCA protein assay kit (ThermoFisher) and examined by Western blot analysis. After SDS-PAGE, proteins were transferred to PVDF membranes (Invitrogen). Membranes were blocked in 5% nonfat dry milk in TBST (50 mM Tris, 0.2% Tween 20, and 150 mM NaCl) for 1h at RT and then incubated overnight at 4°C with primary antibody in blocking buffer. Bands were detected by enhanced chemiluminescence following the manufacturer's protocol (GE Healthcare).

Electrochemiluminescent immunoassay

Cells were cultured on Matrigel in neural induction medium with or without DOX. After 24 h, supernatant was collected and cells were scraped in lysis buffer. WNT3A protein levels were assayed using a Mesoscale Discovery system (MSD) WNT3A kit following the manufacturer's protocol. Plates were analyzed on a SECTOR Imager 6000 instrument with MSD Workbench™ v.3 software. Human WNT3A recombinant protein (R&D Systems) was used as standard.

RNA-Seq data analysis

Total RNA, isolated as described above, was amplified using a Truseq RNA Library preparation kit (Illumina). Sequencing reads were obtained using a NextSeq Sequencing System (Illumina). High quality reads were aligned to the human genome (hg19 assembly) using ran-STAR aligner and reads mapping to each gene were calculated using the HTSeq toolkit. Differential gene expression analysis was carried out through edgeR package (Bioconductor). Genes with a minimum of two-fold expression difference and FDR < 0.01 were considered as differentially expressed.

Chromatin Immunoprecipitation (ChIP)

ChIPs were carried out as previously described [46]. Briefly, at 12 h hESC (1×10^6) with or without GLIS3 induction were cross-linked with 1% formaldehyde in PBS for 8 min at RT, and the reaction was quenched by the addition of glycine at a final concentration of 0.125 M for 8 min at RT. Cells were washed twice with PBS, resuspended in 1ml of cold lysis buffer A (50 mM Hepes, pH7.5; 140 mM NaCl; 1 mM EDTA; 10% glycerol; 0.5% NP-40; 0.25% Triton X-100; 1× complete protease inhibitor cocktail (Roche)), and incubated for 10 min on ice. Cells were then pelleted and resuspended in 1 ml lysis buffer B (10 mM Tris-HCl, pH

8.0; 200 mM NaCl; 1 mM EDTA; 0.5 mM EGTA; 1× protease inhibitor cocktail). After 10 min on ice, cells were sonicated for 10 min in lysis buffer C (10 mM Tris-HCl, pH 8.0; 100 mM NaCl; 1 mM EDTA; 0.5 mM EGTA; 0.5% N-lauroylsarcosine; 1× protease inhibitor cocktail) using a Covaris sonicator to obtain 200–500 bp fragments. After removal of cell debris by centrifugation at 14,000 rpm, chromatin was incubated overnight at 4°C with HA antibody (Cell Signaling), and subsequently incubated for 4 hours with protein A/G-conjugated magnetic beads (Pierce Biotech). The chromatin bound beads were then washed and reverse cross-linked as previously described [47]. ChIP enrichment was evaluated using quantitative PCR as percentage of input and normalized to a negative primer set. ChIP primers are listed in Supporting Information Table S3.

ChIP-Seq data analysis

Single-end 51 bp reads generated from HA-GLIS3 ChIP-seq were aligned to the human reference genome (hg19 assembly) using Bowtie version 0.12.8 [48], and only those reads that mapped to unique genomic locations with at most two mismatches were retained for further analysis. For visualization on the UCSC Genome Brower, and generation of screenshots and read density plots, the data was normalized to reads per million (RPM) and plotted as histograms. For binding site definition (peak call), aligned reads were processed using SISSRs [49, 50] using default settings. Genome-wide distribution of binding sites was determined with reference to RefSeq gene annotations. The proximal GLIS3 regulatory region was defined as GLIS3 binding within 5 kb (upstream or downstream) of TSSs.

Functional and pathway enrichment analysis

Pathway analyses were performed using ConsensusPathDB (http://cpdb.molgen.mpg.de/MCPDB) and REACTOME pathway annotations. Analysis of the GO biological process was performed with David Bioinformatics Resources [51]. A threshold of FDR <1% or p value < 0.01 was used to select for statistically significant categories.

Motif analysis

Relevant sequences spanning 200 nucleotides around the centers of GLIS3 binding sites were retrieved from the reference genome and *de novo* motif search was performed using MEME [52] using zoops (zero or one motif occurrence per sequence) option.

Statistical analysis

Data were expressed as mean and standard error of mean (SEM). Statistical significance was determined by unpaired two-tailed Student's *t*-test or analysis of variance (ANOVA) with Sidak's multiple comparisons test to examine whether there are significant differences among the levels using R version 3.4.0. All results were derived from three or more independent experiments.

RESULTS

Induction of NPC differentiation in hESCs containing a DOX-inducible GLIS3

To investigate GLIS3 function during neural development, we generated stable H9 hESC lines expressing a DOX-inducible GLIS3, referred to as G3-hESCs, that allow induction of GLIS3 by addition of DOX in the culture medium (Fig. 1A). These stable G3-hESC lines maintained the characteristic morphological features of undifferentiated hESCs and expressed the hESC markers, OCT4, TRA 1–81, SOX2, and NANOG, at levels comparable to that of wild-type hESCs (Supporting Information Fig. S1A and B). FACS analysis confirmed that 98% and 96.8% of G3-hESCs stained positive for OCT4 and TRA 1–81, respectively (Supporting Information Fig. S1C).

To induce differentiation of hESCs into neural progenitor cells (NPCs), we employed a previously validated system that directs differentiation of hESCs into NPCs over seven days [41–43] (Fig. 1B). To induce NPC differentiation, G3-hESCs were plated in Matrigel-coated dishes and grown for 24 h in mTeSR1 medium before medium was switched to DMEM/B27 medium supplemented with activin/TGFβ/BMP pathway inhibitors. NPC differentiation was examined in G3-hESCs treated with or without DOX (referred to as G3-hESC(+) and G3-hESC(−), respectively). *GLIS3* mRNA was rapidly induced upon the addition of DOX (Fig. 1C). Immunocytochemical staining with an anti-Flag antibody showed that ~82% of the cells stained positive for Flag-GLIS3 at 12 h after the addition of DOX (Fig. 1D and Supporting Information Fig. S2A). Both G3-hESCs(−) and G3-hESCs(+) efficiently differentiated into NPCs, referred to as G3-NPCs(−) and G3-NPCs(+), respectively, as evident from the loss of the typical hESC morphology and appearance of the NPC morphology (Supporting Information Fig. S2B). NPC differentiation in G3-NPCs(−) and G3-NPCs(+) was supported by the increased expression of the signature neural markers, *SOX1*, *NCAM*, and *NESTIN* (Fig. 1E). NPC differentiation was confirmed by immunocytochemical staining and FACS analysis, which showed that more than 90% of the cells stained positive for SOX1, NESTIN, and NCAM protein (Fig. 1F and G, Supporting Information Fig. S2C). Consistent with NPC differentiation, endoderm lineage marker genes, including *SOX17* and *FOXA2*, and mesoderm markers, such as *HAND1* and *MIXL1*, were not induced during either G3-NPC(−) or G3-NPC(+) differentiation (Supporting Information Table S4).

GLIS3 regulates anterior-posterior specification in hESC-derived NPCs

hESCs cells undergoing neural differentiation acquire, by default, an anterior NPC fate that is associated with increased expression of anterior-specific genes, such as the transcription factors *PAX6*, *OTX1* and *ZIC1* [15, 53–55]. Interestingly, unlike the induction of *PAX6* mRNA in G3-NPCs(−), the induction of neural differentiation in G3-NPCs(+) was not accompanied by increased *PAX6* expression (Fig. 2A). FACS analysis showed that, in contrast to G3-NPCs(−), which are ~75% positive for PAX6, <2% of the G3-NPCs(+) were PAX6 positive at day 7 of NPC differentiation (Fig. 2B). The lack of PAX6 induction in G3-NPCs(+) suggested a potential regulatory role for GLIS3 in A-P lineage specification.

Consistent with this hypothesis, examination of expression of additional A-P patterning-associated genes during differentiation of G3-hESCs into NPCs revealed that, in addition to *PAX6*, several other anterior phenotype-associated genes, including *OTX1* and *ZIC1*, as well as *OTX2*, which are expressed at the forebrain/midbrain boundary, were not induced in cells expressing GLIS3 (Fig. 2C). Instead, G3-NPC(+) cells expressed high levels of several posterior NPC marker genes, including *GBX2*, *KROX20*, *HOXA, NKX6–2*, and *MNX1* (Fig. 2D). These diametrically opposite expression patterns of A-P marker genes in G3-NPCs(−) and G3-NPCs(+) were validated by immunocytochemical staining, wherein most G3-NPCs(−) cells, 5 days post-NPC induction, stained positive for the anterior markers OTX2 and PAX6, but not for the posterior markers GBX2 and MNX1 (Fig. 2E). In contrast, most G3-NPCs(+) stained positive for GBX2 and MNX1, but not for OTX2 and PAX6 (Fig. 2E). Quantitation by FACS analysis showed that at day 5 post-NPC induction 85.2% and 67.7% of the G3-NPCs(−) were positive for OTX2 (Fig. 2F) and PAX6 (Fig. 2G), respectively, whereas <1% of the cells were GBX2-positive (Fig. 2F). The opposite was observed for G3-NPCs(+), where <0.1% and <1.2% of the cells were positive for OTX2 and PAX6 respectively, whereas 93.2% of the cells were positive for GBX2 (Fig. 2F,G).

To ensure that our findings are not specific to the cell line used (H9 hESCs), we repeated our experiments using a different hESC line (H1 hESCs) stably expressing DOX-inducible GLIS3 (referred to as G3-H1-hESCs). G3-H1-hESCs express hESC markers, OCT4, SOX2, and NANOG, at levels comparable to that of wild-type H1 hESCs (Supporting Information Fig. S3A). Similar to our findings using H9 hESCs, expression of GLIS3 in H1 hESCs induced posterior NPC differentiation, as indicated by the suppression of the anterior markers (Supporting Information Fig. S3B) and induction of posterior NPC markers (Supporting Information Fig. S3C). Altogether, these data are consistent with a regulatory role for GLIS3 in promoting the posterior lineage in hESC-derived NPCs in lieu of the default anterior NPC fate (Fig. 2H).

GLIS3-mediated posterior specification involves extracellular signaling

Several morphogens, including retinoic acid (RA), bone morphogenetic proteins (BMPs), fibroblast growth factors (FGFs), and WNT proteins, have been implicated in the paracrine or autocrine regulation of A-P neural patterning [16–24]. To determine whether the GLIS3-mediated shift from anterior to posterior NPC fate involved synthesis and secretion of posteriorizing factors, we investigated whether conditioned media derived from GLIS3-expressing G3-hESC(+) cultures, had an effect on A-P axis specification of wild-type hESCs. Indeed, culturing wild-type hESCs in the presence of conditioned media derived from G3-hESC(+) cultures, induced differentiation of hESCs into NPCs with a posterior fate, as evidenced by the induction of the posterior markers, *GBX2*, *MNX1*, and *HOXA2*, and repression of the anterior markers, *OTX2*, *PAX6*, and *ZIC1* (Fig. 3A, 3B). These observations suggested that GLIS3-induced posteriorization of the neural fate in hESCs involves an autocrine or paracrine signaling pathway.

GLIS3 activates WNT genes and WNT signaling-associated targets

To gain insights into the mechanism by which GLIS3 regulates A-P regional identity and to elucidate signaling pathways and gene expression programs regulated by GLIS3, we

employed RNA-Seq to profile global gene expression changes at various time points during G3-hESC to NPC differentiation (0 h, 12 h, 1, 2, 3, and 7 days), in the presence or absence of DOX. RNA-Seq data further confirmed the induction of several posterior fate-associated genes, such as *GBX2*, *CDX1*, *CDX2*, *MSX1*, *MNX1*, *PAX2*, and *NRGN*, in differentiating G3-hESCs(+) (Fig. 4A, Supporting Information Fig. S4 and Table S4); in contrast, the expression of anterior fate-associated genes, such as *OTX1*, *ZIC1*, *LHX5*, *LHX6*, *PAX6*, *DXL4*, *HHEX*, and *SIX2*, and several midbrain-associated genes, including *OTX2*, *EN1*, *SIX3*, and *LHX1* were largely suppressed.

To separate the cause from the effect, we focused on gene expression changes at 12 h into NPC differentiation and found that nearly 1,000 genes were significantly up/down-regulated in differentiating G3-hESCs(+) compared to differentiating G3-hESCs(−). Pathway analysis revealed an enrichment for WNT signaling genes among those upregulated in G3-NPCs(+) (Fig. 4B and Supporting Information Table S5), which is consistent with established roles for WNT signaling in the initial A-P NPC differentiation of hESCs and in the patterning of the neural tube [8, 9, 16, 18, 21, 23, 24]. Examination of the gene expression profiles of WNT pathway-associated components confirmed the induction of several WNT genes, including *WNT2B*, *WNT3*, *WNT3A*, *WNT7A*, and *WNT8A*, and their receptors *FZD10* and *FZD9*, during NPC differentiation of G3-hESCs(+) (Fig. 4C). In contrast to the induction of many posterior marker genes (Fig. 2D and 4A), WNT genes are induced as early as 12h of G3-NPC(+) differentiation (Fig. 4C). To determine whether elevated levels of WNT pathway-associated genes in differentiating G3-hESCs(+) were accompanied by activation of the WNT signaling pathway, we examined the expression of several downstream targets. As shown in (Fig. 4C), a number of WNT target genes, including *TCF7*, *LEF1*, *SP5*, and *AXIN2*, were (transiently) upregulated in differentiating G3-hESCs(+). Collectively, these data suggest that increased GLIS3 expression leads to activation of the WNT signaling pathway through the direct or indirect induction of WNT gene expression.

WNT genes are direct transcriptional targets of GLIS3

GLIS3 is known to activate transcription of its target genes by binding to cis-regulatory elements (GLIS3 binding sites) [27, 28, 56]. To determine whether GLIS3 regulates the transcription of any of the WNT pathway-associated genes directly, we performed ChIP-Seq analysis to map genome-wide occupancy of exogenous, HA-tagged GLIS3 in G3-hESCs(+) after 12 h of NPC induction when GLIS3 is well expressed (Fig. 1C, 1D), using an antibody against HA. As a control, we performed ChIP-Seq analysis in G3-hESCs(−), which do not express HA-GLIS3 (Fig. 1D). Our analysis of the ChIP-Seq data, using SISSRs peak calling algorithm [49, 50], identified a total of 18,785 GLIS3 binding sites in G3-hESCs(+) and just 79 peaks in G3-hESCs(−) (Fig. 5A, 5B). Consistent with our previous finding in mouse thyroid glands [28], about two-thirds of all GLIS3 binding sites are located within intragenic regions or immediately upstream (5 Kb) of transcription start sites, consistent with a role for GLIS3 in transcriptional regulation (Fig. 5C). *De novo* sequence motif analysis of GLIS3 binding sites identified a G-rich consensus sequence, similar to the consensus obtained from ChIP-Seq studies in mouse thyroid gland [28] and the GLIS3 binding motif we previously identified using an *in vitro* binding assay [57](Fig. 5D). Gene Ontology (GO) analysis of GLIS3-target genes revealed an enrichment for genes associated with transcriptional

regulation, WNT signaling, and neural development/differentiation (Fig. 5E and Supporting Information Table S6).

Comparison of genes targeted by GLIS3 with those induced or suppressed in G3-hESCs(+) at 12 h of NPC induction, revealed that about one-third of the upregulated genes are GLIS3 targets (P-value = 1.53E-13; hypergeometric test), whereas only ~9% of the downregulated genes bind GLIS3 (P-value = 0.99), consistent with GLIS3's proposed role as a transcriptional activator [25, 27, 28, 56, 57]. Gene Ontology (GO) analysis of genes that were both targeted by GLIS3 and upregulated during NPC differentiation, revealed enrichment for genes associated with WNT signaling, embryonic development, and A-P axis specification (Fig. 5E and Supporting Information Table S6). Notably, several genes associated with the WNT signaling pathway and A-P axis neural specification, including *WNT3A*, *WNT3*, *WNT7A*, *WNT10A*, *WNT11* and the WNT receptor *FZD10* (Fig. 5F, Supporting Information Fig. S5 and Table S7), which were significantly upregulated during NPC induction, are GLIS3 targets. Together, these data suggest a critical role for GLIS3 in the transcriptional activation of key WNT signaling-associated genes, previously implicated in the regulation of A-P patterning [8, 9, 16, 18, 21, 23, 24, 58].

GLIS3 regulates WNT3A transcription

To directly test GLIS3's ability to transcriptionally activate WNT genes, we investigated the transactivation dynamics of *WNT3A*, which is induced in differentiating G3-hESCs(+), as early as 6 h into NPC induction (Fig. 5G and Supporting Information Fig. S4), soon after GLIS3 expression (Fig. 1C, 1D), but well before the induction of many posterior markers (Fig. 2D). We confirmed this observation using G3-H1-hESCs(+) (Supporting Information Fig. S6A). WNT3A has been reported to play a critical role in the regulation of A-P patterning and the posteriorization of the neural tube [8, 9, 18, 21, 58, 59]. After validating GLIS3 binding at the *WNT3A* promoter by ChIP-qPCR (Supporting Information Fig. S6B), we examined whether GLIS3 was able to activate the *WNT3A* promoter in a reporter assay, wherein the luciferase expression is under the control of the *WNT3A* promoter, which contains several GLIS3 binding sites (Supporting Information Fig. S6C). DOX-inducible GLIS3 was able to enhance luciferase reporter activity in G3-hESCs as well as in G3-HEK293 cells in DOX-dependent manner (Fig. 5H). Furthermore, the increase in luciferase activity positively correlated with GLIS3 protein levels ($R^2 = 0.97$) (Fig. 5I). Together, these data are consistent with the conclusion that GLIS3 can activate *WNT3A* transcription.

GLIS3-mediated posterior specification is WNT-dependent

To determine whether GLIS3-mediated posterior specification of NPCs was dependent on the activation of the WNT signaling pathways and the increase in *WNT3A* expression in particular, we first confirmed that the induction of *WNT3A* mRNA expression in G3-hESCs(+) (Fig. 5G) was accompanied by an increase in WNT3A protein levels (Fig. 5J). ELISA analysis confirmed the dramatic increase in the levels of both cellular and secreted WNT3A in G3-hESCs(+) and conditioned medium, respectively (Fig. 5K). To determine whether GLIS3-mediated posteriorization was WNT-dependent, we examined the effect of two WNT inhibitors, WNT-C59 and IWP2, on the differentiation of G3-hESCs(+) into posterior NPCs. These two inhibitors inhibit the activity of the membrane-bound,

acyltransferase Porcupine (PORCN), which is required for WNT palmitoylation, secretion, and activity [60, 61]. Remarkably, both WNT-C59 and IWP2 significantly inhibited the induction of posterior markers and abrogated the suppression of anterior markers in GLIS3-expressing NPCs (Fig. 6A). Immunocytochemical staining further confirmed the suppression of posterior specification in GLIS3-expressing cells by WNT inhibitors (Fig. 6B). The number of GBX2 and MNX1 positive cells, marking posterior fate, is greatly reduced in cells treated with WNT-C59 or IWP2, with a concomitant increase in the number of OTX2 and PAX6 positive cells, which mark the anterior fate. These data suggested that GLIS3-mediated posterior specification is WNT-dependent. Addition of recombinant WNT3A during differentiation of G3-hESCs(−) into NPCs induced posterior markers and suppressed anterior markers to a similar extent to that observed in NPCs derived from G3-hESCs(+) (Fig. 6C and Supporting Information Fig. S7). Collectively, these observations support the conclusion that GLIS3-mediated posterior specification is at least in part through synthesis and secretion of WNT proteins and WNT3A in particular.

DISCUSSION

Regional specification along the antero-posterior (A-P) axis during which the neural tube becomes subdivided into several subregions that will develop into the forebrain, midbrain, hindbrain, and spinal cord, is one of the most important events during early brain development in vertebrates. Although recent studies have shed significant insights into signaling pathways that regulate A-P patterning, much of the molecular mechanisms that underlie these controls remain still poorly understood. According to the double-gradient model for the regulation of neural tube patterning [62], ectodermal cells, upon acquisition of neural identity, acquire anterior fates, which then posteriorize under the influence of various paracrine and autocrine signaling pathways, including the BMP, retinoic acid, FGF, and WNT pathways [4, 8–10, 16, 18, 19, 21–24, 55, 63, 65]. Consistent with this model, directed neural differentiation of hESCs, by default, drives the cells along the anterior NPC lineage. In this study, we show that increased expression of GLIS3 induces differentiation of hESCs along the posterior NPC lineage, in lieu of the default anterior NPC fate, as indicated by the suppression of anterior marker gene expression and the induction of posterior markers (Fig. 7). The posterior NPCs derived from G3-hESCs(+) are multipotential and able to differentiate further in astrocytes and different neuronal lineages (data not shown) as one would predict.

Previous studies have shown that A-P neural patterning is regulated by a morphogen gradient of WNT/β-catenin signaling [3, 4, 10–13, 16, 18, 21, 58] and identified WNT3A as a major posteriorizing factor that by itself is able to steer posterior NPC lineage differentiation in hESCs [18, 21]. In the canonical WNT pathway, interaction of WNT3A with Frizzled receptors leads to stabilization and nuclear translocation of β-catenin, which then forms a complex with LEF/TCF transcription factors that subsequently activate the transcription of target genes, such as *SP5* and *AXIN2*, and several posterior markers, including certain *HOX* genes [2, 4, 21, 64]. In this study, we identify a potential role for GLIS3 in the regulation of A-P lineage specification (Fig. 7). Our data suggest that the induction of posterior NPC differentiation is mediated by a GLIS3-induced activation of WNT signaling pathway. This conclusion is supported by data showing that GLIS3 induces

the expression of a number of WNT signaling genes, including *WNT3A*, *WNT3*, *WNT8A*, *WNT11*, and their receptors, *FZD1* and *FZD10* (Fig. 4C and Fig. 5G), and markedly increases the synthesis and secretion of the strong posteriorizing factor WNT3A (Fig. 5J and 5K) [8, 9, 18, 21, 58, 59]. These data suggest that GLIS3-mediated posterior neural identity in hESCs is at least in part mediated by WNT3A (Fig. 7). In contrast to WNT3A, the expression of several WNT antagonists (*WIF1, FRZB*, and *DKK3*; Fig. 4C) was decreased in GLIS3-induced NPCs. These observations suggest that, in addition to GLIS3-mediated activation of WNT genes, suppression of WNT antagonists may also be contribute to GLIS3-mediated induction of posterior neural identity. This interpretation is consistent with previous studies showing that increased expression of WNT antagonists promote anterior neural lineage differentiation, while inhibiting the posterior lineage [21].

Although WNT3A is a strong posteriorizing factor in hESCs, the neural tube is still being formed in the absence of WNT3A expression [8, 66–68]. Likewise, GLIS3-deficiency does not have an obvious effect on neural tube formation (unpublished observations). This might be due to redundancy between the different morphogen pathways controlling A-P patterning *in vivo* and the different transcription factors regulating them. This is supported by studies showing that in addition to WNT signaling, several other paracrine and autocrine mechanisms have been implicated in the regulation of A-P neural patterning, including the FGF and retinoid pathways [11, 18, 19, 22–24, 63, 65]. FGF2 in particular, and FGF4 and FGF8 to a lesser extent, have been reported to promote posterior differentiation, whereas the effect of other FGFs is unknown. Although expression of *FGF8*, *FGF10*, and *FGF17* is elevated in differentiating G3-hESCs(+), their induction occurs late (at day 3 or 7) compared to that of WNT genes (Fig. 4A, 4B) suggesting that it is less likely that FGFs play an active role in the initial phase of GLIS3-mediated posteriorization in hESCs.

Although WNT signaling is known to play a critical role in A-P patterning, our understanding of the mechanisms that regulate *WNT* gene expression is still incomplete. We reported previously that GLIS3 regulates transcription by binding to GLIS binding sites (GLISBS) in the promoter region of target genes [27, 28, 31]. Our ChIP-Seq and functional studies show that GLIS3 binds to and transcriptionally activates several WNT genes, including *WNT3A* (Fig. 5), indicating that GLIS3 functions as an upstream regulator of *WNT3A* transcription. Our ChIP-Seq data (Supporting Information Table S6) further revealed that, in addition to *WNT* genes, GLIS3 binds to several genes encoding transcription factors that are important in regulating neural identity, including *GBX2*, *CDX1*, and *MNX1*. Since GBX2 has been reported to regulate mid- and hindbrain specification by directly repressing the transcription of the homeobox transcription factor *OTX2*, which is expressed in the fore/midbrain region [14], the suppression of OTX2 expression during GLIS3-induced posterior NPC differentiation may be in part due to the induction of GBX2.

In summary, our study shows that the transcription factor GLIS3 can direct posterior NPC specification of human ESC-derived NPCs in lieu of the default anterior fate and demonstrates that this is mediated through GLIS3-mediated transcriptional activation of an autocrine WNT3A pathway (Fig. 7). Induction of GLIS3 in ESCs provides a source of posterior NPCs that will be valuable in the further study of the differentiation and function of these cells and the role of GLIS3 in neural development, as well as provide greater

insights into the various neurodegenerative disorders, such as mild mental retardation and increased risk of Parkinson's and Alzheimer's disease, in which GLIS3 has been implicated.

Supplementary Material

Refer to Web version on PubMed Central for supplementary material.

ACKNOWLEDGMENTS

We thank Carl D. Bortner for help with the FACS analysis and Mi Kyeong Lee for help with ANOVA analysis. This research was supported by the Intramural Research Program of the National Institute of Environmental Health Sciences, the National Institutes of Health, Z01-ES-100485 to AMJ and Z01ES102625 to RJ.

REFERENCES

1. Elkouby YM, Frank D. Wnt/beta-Catenin Signaling in Vertebrate Posterior Neural Development In: Kessler DS, editor. Colloquium Series on Developmental Biology. San Rafael, CA: Morgan & Claypool Life Sciences; 2010.
2. Inestrosa NC, Arenas E. Emerging roles of Wnts in the adult nervous system. Nat Rev Neurosci. 2010;11:77–86. [PubMed: 20010950]
3. Roelink H, Nusse R. Expression of two members of the Wnt family during mouse development--restricted temporal and spatial patterns in the developing neural tube. Genes Dev. 1991;5:381–388. [PubMed: 2001840]
4. Ciani L, Salinas PC. WNTs in the vertebrate nervous system: from patterning to neuronal connectivity. Nat Rev Neurosci. 2005;6:351–362. [PubMed: 15832199]
5. Fancy SP, Baranzini SE, Zhao C, et al. Dysregulation of the Wnt pathway inhibits timely myelination and remyelination in the mammalian CNS. Genes Dev. 2009;23:1571–1585. [PubMed: 19515974]
6. Ille F, Sommer L. Wnt signaling: multiple functions in neural development. Cell Mol Life Sci. 2005;62:1100–1108. [PubMed: 15928805]
7. Pei Y, Brun SN, Markant SL, et al. WNT signaling increases proliferation and impairs differentiation of stem cells in the developing cerebellum. Development. 2012;139:1724–1733. [PubMed: 22461560]
8. Garriock RJ, Chalamalasetty RB, Kennedy MW, et al. Lineage tracing of neuromesodermal progenitors reveals novel Wnt-dependent roles in trunk progenitor cell maintenance and differentiation. Development. 2015;142:1628–1638. [PubMed: 25922526]
9. Braun MM, Etheridge A, Bernard A, et al. Wnt signaling is required at distinct stages of development for the induction of the posterior forebrain. Development. 2003;130:5579–5587. [PubMed: 14522868]
10. Blauwkamp TA, Nigam S, Ardehali R, et al. Endogenous Wnt signalling in human embryonic stem cells generates an equilibrium of distinct lineage-specified progenitors. Nat Commun. 2012;3:1070. [PubMed: 22990866]
11. Wassarman KM, Lewandoski M, Campbell K, et al. Specification of the anterior hindbrain and establishment of a normal mid/hindbrain organizer is dependent on Gbx2 gene function. Development. 1997;124:2923–2934. [PubMed: 9247335]
12. Augustine K, Liu ET, Sadler TW. Antisense attenuation of Wnt-1 and Wnt-3a expression in whole embryo culture reveals roles for these genes in craniofacial, spinal cord, and cardiac morphogenesis. Dev Genet. 1993;14:500–520. [PubMed: 8111977]
13. Liu P, Wakamiya M, Shea MJ, et al. Requirement for Wnt3 in vertebrate axis formation. Nat Genet. 1999;22:361–365. [PubMed: 10431240]
14. Inoue F, Kurokawa D, Takahashi M, et al. Gbx2 directly restricts Otx2 expression to forebrain and midbrain, competing with class III POU factors. Mol Cell Biol. 2012;32:2618–2627. [PubMed: 22566684]

15. Schwarz M, Alvarez-Bolado G, Dressler G, et al. Pax2/5 and Pax6 subdivide the early neural tube into three domains. Mech Dev. 1999;82:29–39. [PubMed: 10354469]
16. Yamaguchi TP. Heads or tails: Wnts and anterior-posterior patterning. Curr Biol. 2001;11:R713–724. [PubMed: 11553348]
17. Harada H, Sato T, Nakamura H. Fgf8 signaling for development of the midbrain and hindbrain. Dev Growth Differ. 2016;58:437–445. [PubMed: 27273073]
18. Hendrickx M, Van XH, Leyns L. Anterior-posterior patterning of neural differentiated embryonic stem cells by canonical Wnts, Fgfs, Bmp4 and their respective antagonists. Dev Growth Differ. 2009;51:687–698. [PubMed: 19703209]
19. Pera EM, Acosta H, Gouignard N, et al. Active signals, gradient formation and regional specificity in neural induction. Exp Cell Res. 2014;321:25–31. [PubMed: 24315941]
20. Osakada F, Takahashi M. Neural induction and patterning in Mammalian pluripotent stem cells. CNS Neurol Disord Drug Targets. 2011;10:419–432. [PubMed: 21495966]
21. Moya N, Cutts J, Gaasterland T, et al. Endogenous WNT signaling regulates hPSC-derived neural progenitor cell heterogeneity and specifies their regional identity. Stem Cell Reports. 2014;3:1015–1028. [PubMed: 25458891]
22. Kudoh T, Wilson SW, Dawid IB. Distinct roles for Fgf, Wnt and retinoic acid in posteriorizing the neural ectoderm. Development. 2002;129:4335–4346. [PubMed: 12183385]
23. Kiecker C, Niehrs C. A morphogen gradient of Wnt/beta-catenin signalling regulates anteroposterior neural patterning in Xenopus. Development. 2001;128:4189–4201. [PubMed: 11684656]
24. Nordstrom U, Jessell TM, Edlund T. Progressive induction of caudal neural character by graded Wnt signaling. Nat Neurosci. 2002;5:525–532. [PubMed: 12006981]
25. Kim YS, Nakanishi G, Lewandoski M, et al. GLIS3, a novel member of the GLIS subfamily of Kruppel-like zinc finger proteins with repressor and activation functions. Nucleic Acids Res. 2003;31:5513–5525. [PubMed: 14500813]
26. Kang HS, ZeRuth G, Lichti-Kaiser K, et al. Gli-similar (Glis) Krüppel-like zinc finger proteins: insights into their physiological functions and critical roles in neonatal diabetes and cystic renal disease. Histol Histopath. 2010;25:1481–1496.
27. Lichti-Kaiser K, ZeRuth G, Kang HS, et al. Gli-similar proteins: their mechanisms of action, physiological functions, and roles in disease. Vitam Horm. 2012;88:141–171. [PubMed: 22391303]
28. Kang HS, Kumar D, Liao G, et al. GLIS3 is indispensable for TSH/TSHR-dependent thyroid hormone biosynthesis and follicular cell proliferation. J Clin Invest. 2017;127:4326–4337. [PubMed: 29083325]
29. Kang HS, Takeda Y, Jeon K, et al. The Spatiotemporal Pattern of Glis3 Expression Indicates a Regulatory Function in Bipotent and Endocrine Progenitors during Early Pancreatic Development and in Beta, PP and Ductal Cells. PLoS One. 2016;11:e0157138. [PubMed: 27270601]
30. Kang HS, Chen LY, Lichti-Kaiser K, et al. Transcription Factor GLIS3: A New and Critical Regulator of Postnatal Stages of Mouse Spermatogenesis. Stem Cells. 2016;34:2772–2783. [PubMed: 27350140]
31. Jetten AM. GLIS1–3 transcription factors: critical roles in the regulation of multiple physiological processes and diseases. Cell Mol Life Sci. 2018.
32. Lee SY, Noh HB, Kim HT, et al. Glis family proteins are differentially implicated in the cellular reprogramming of human somatic cells. Oncotarget. 2017;8:77041–77049. [PubMed: 29100368]
33. Scoville DW, Kang HS, Jetten AM. GLIS1–3: emerging roles in reprogramming, stem and progenitor cell differentiation and maintenance. Stem Cell Investig. 2017;4:80.
34. Senee V, Chelala C, Duchatelet S, et al. Mutations in GLIS3 are responsible for a rare syndrome with neonatal diabetes mellitus and congenital hypothyroidism. Nat Genet. 2006;38:682–687. [PubMed: 16715098]
35. Dimitri P, Warner JT, Minton JA, et al. Novel GLIS3 mutations demonstrate an extended multisystem phenotype. Eur J Endocrinol. 2011;164:437–443. [PubMed: 21139041]

36. Chung SJ, Kim MJ, Kim J, et al. Association of type 2 diabetes GWAS loci and the risk of Parkinson's and Alzheimer's diseases. Parkinsonism Relat Disord. 2015;21:1435–1440. [PubMed: 26499758]
37. Cruchaga C, Kauwe JS, Harari O, et al. GWAS of cerebrospinal fluid tau levels identifies risk variants for Alzheimer's disease. Neuron. 2013;78:256–268. [PubMed: 23562540]
38. Dimitri P, Habeb AM, Gurbuz F, et al. Expanding the Clinical Spectrum Associated With GLIS3 Mutations. J Clin Endocrinol Metab. 2015;100:E1362–1369. [PubMed: 26259131]
39. Calderari S, Ria M, Gerard C, et al. Molecular genetics of the transcription factor GLIS3 identifies its dual function in beta cells and neurons. Genomics. 2017;110:98–111. [PubMed: 28911974]
40. Lukashova-v Zangen I, Kneitz S, Monoranu CM, et al. Ependymoma gene expression profiles associated with histological subtype, proliferation, and patient survival. Acta Neuropathol (Berl). 2007;113:325–337. [PubMed: 17265049]
41. Chen KG, Mallon BS, Hamilton RS, et al. Non-colony type monolayer culture of human embryonic stem cells. Stem Cell Res. 2012;9:237–248. [PubMed: 22910561]
42. Zhou J, Su P, Li D, et al. High-efficiency induction of neural conversion in human ESCs and human induced pluripotent stem cells with a single chemical inhibitor of transforming growth factor beta superfamily receptors. Stem Cells. 2010;28:1741–1750. [PubMed: 20734356]
43. Surmacz B, Fox H, Gutteridge A, et al. Directing differentiation of human embryonic stem cells toward anterior neural ectoderm using small molecules. Stem Cells. 2012;30:1875–1884. [PubMed: 22761025]
44. Meerbrey KL, Hu G, Kessler JD, et al. The pINDUCER lentiviral toolkit for inducible RNA interference in vitro and in vivo. Proc Natl Acad Sci U S A. 2011;108:3665–3670. [PubMed: 21307310]
45. Livak KJ, Schmittgen TD. Analysis of relative gene expression data using real-time quantitative PCR and the 2(-Delta Delta C(T)) Method. Methods. 2001;25:402–408. [PubMed: 11846609]
46. Oldfield AJ, Yang P, Conway AE, et al. Histone-fold domain protein NF-Y promotes chromatin accessibility for cell type-specific master transcription factors. Mol Cell. 2014;55:708–722. [PubMed: 25132174]
47. Heard E, Rougeulle C, Arnaud D, et al. Methylation of histone H3 at Lys-9 is an early mark on the × chromosome during × inactivation. Cell. 2001;107:727–738. [PubMed: 11747809]
48. Langmead B, Trapnell C, Pop M, et al. Ultrafast and memory-efficient alignment of short DNA sequences to the human genome. Genome Biol. 2009;10:R25. [PubMed: 19261174]
49. Jothi R, Cuddapah S, Barski A, et al. Genome-wide identification of in vivo protein-DNA binding sites from ChIP-Seq data. Nucleic Acids Res. 2008;36:5221–5231. [PubMed: 18684996]
50. Narlikar L, Jothi R. ChIP-Seq data analysis: identification of protein-DNA binding sites with SISSRs peak-finder. Methods Mol Biol. 2012;802:305–322. [PubMed: 22130889]
51. Huang da W, Sherman BT, Lempicki RA. Systematic and integrative analysis of large gene lists using DAVID bioinformatics resources. Nat Protoc. 2009;4:44–57. [PubMed: 19131956]
52. Bailey TL, Elkan C. Fitting a mixture model by expectation maximization to discover motifs in biopolymers. Proc Int Conf Intell Syst Mol Biol. 1994;2:28–36. [PubMed: 7584402]
53. Schmahl W, Knoedlseder M, Favor J, et al. Defects of neuronal migration and the pathogenesis of cortical malformations are associated with Small eye (Sey) in the mouse, a point mutation at the Pax-6-locus. Acta Neuropathol. 1993;86:126–135. [PubMed: 8213068]
54. Walther C, Gruss P. Pax-6, a murine paired box gene, is expressed in the developing CNS. Development. 1991;113:1435–1449. [PubMed: 1687460]
55. Pankratz MT, Li XJ, Lavaute TM, et al. Directed neural differentiation of human embryonic stem cells via an obligated primitive anterior stage. Stem Cells. 2007;25:1511–1520. [PubMed: 17332508]
56. ZeRuth GT, Takeda Y, Jetten AM. The Kruppel-like protein Gli-similar 3 (Glis3) functions as a key regulator of insulin transcription. Mol Endocrinol. 2013;27:1692–1705. [PubMed: 23927931]
57. Beak JY, Kang HS, Kim YS, et al. Functional analysis of the zinc finger and activation domains of Glis3 and mutant Glis3(NDH1). Nucleic Acids Res. 2008;36:1690–1702. [PubMed: 18263616]

58. Dunty WC, Jr., Biris KK, Chalamalasetty RB, et al. Wnt3a/beta-catenin signaling controls posterior body development by coordinating mesoderm formation and segmentation. Development. 2008;135:85–94. [PubMed: 18045842]

59. Fonar Y, Gutkovich YE, Root H, et al. Focal adhesion kinase protein regulates Wnt3a gene expression to control cell fate specification in the developing neural plate. Mol Biol Cell. 2011;22:2409–2421. [PubMed: 21551070]

60. Proffitt KD, Madan B, Ke Z, et al. Pharmacological inhibition of the Wnt acyltransferase PORCN prevents growth of WNT-driven mammary cancer. Cancer Res. 2013;73:502–507. [PubMed: 23188502]

61. Chen B, Dodge ME, Tang W, et al. Small molecule-mediated disruption of Wnt-dependent signaling in tissue regeneration and cancer. Nat Chem Biol. 2009;5:100–107. [PubMed: 19125156]

62. Nieuwkoop P. Activation and organization of the central nervous system. III. Synthesis of a new working hypothesis. J Exp Zool. 1952;120:83–108.

63. Lohnes D. The Cdx1 homeodomain protein: an integrator of posterior signaling in the mouse. Bioessays. 2003;25:971–980. [PubMed: 14505364]

64. van de Ven C, Bialecka M, Neijts R, et al. Concerted involvement of Cdx/Hox genes and Wnt signaling in morphogenesis of the caudal neural tube and cloacal derivatives from the posterior growth zone. Development. 2011;138:3451–3462. [PubMed: 21752936]

65. Lee SM, Danielian PS, Fritzsch B, et al. Evidence that FGF8 signalling from the midbrain-hindbrain junction regulates growth and polarity in the developing midbrain. Development. 1997;124:959–969. [PubMed: 9056772]

66. Yoshikawa Y, Fujimori T, McMahon AP, et al. Evidence that absence of Wnt-3a signaling promotes neuralization instead of paraxial mesoderm development in the mouse. Dev Biol. 1997;183:234–242. [PubMed: 9126297]

67. Kondoh H, Takada S, Takemoto T. Axial level-dependent molecular and cellular mechanisms underlying the genesis of the embryonic neural plate. Dev Growth Differ. 2016;58:427–436. [PubMed: 27279156]

68. Takada S, Stark KL, Shea MJ, et al. Wnt-3a regulates somite and tailbud formation in the mouse embryo. Genes Dev. 1994;8:174–189. [PubMed: 8299937]

SIGNIFICANCE STATEMENT

Neural progenitor cells (NPC) are derived from embryonic stem cells (ESC) during early development of the nervous system and provide a source for a variety of specialized neurons, astrocytes, and oligodendrocytes that form the functioning brain. WNT signaling and WNT proteins are critical in regulating various neural lineages, including the differentiation of ESCs along the posterior NPC lineage. Here, we show that the transcription factor GLI-Similar 3 (GLIS3) can directs posterior NPC specification of human ESC-derived NPCs in lieu of the default anterior fate. This lineage determination is facilitated through GLIS3-mediated transcriptional activation of WNT3A pathway. Induction of GLIS3 in ESCs provides a source of posterior NPCs that will be valuable in the further study of the differentiation and function of these cells, as well as that of various neurodegenerative disorders.

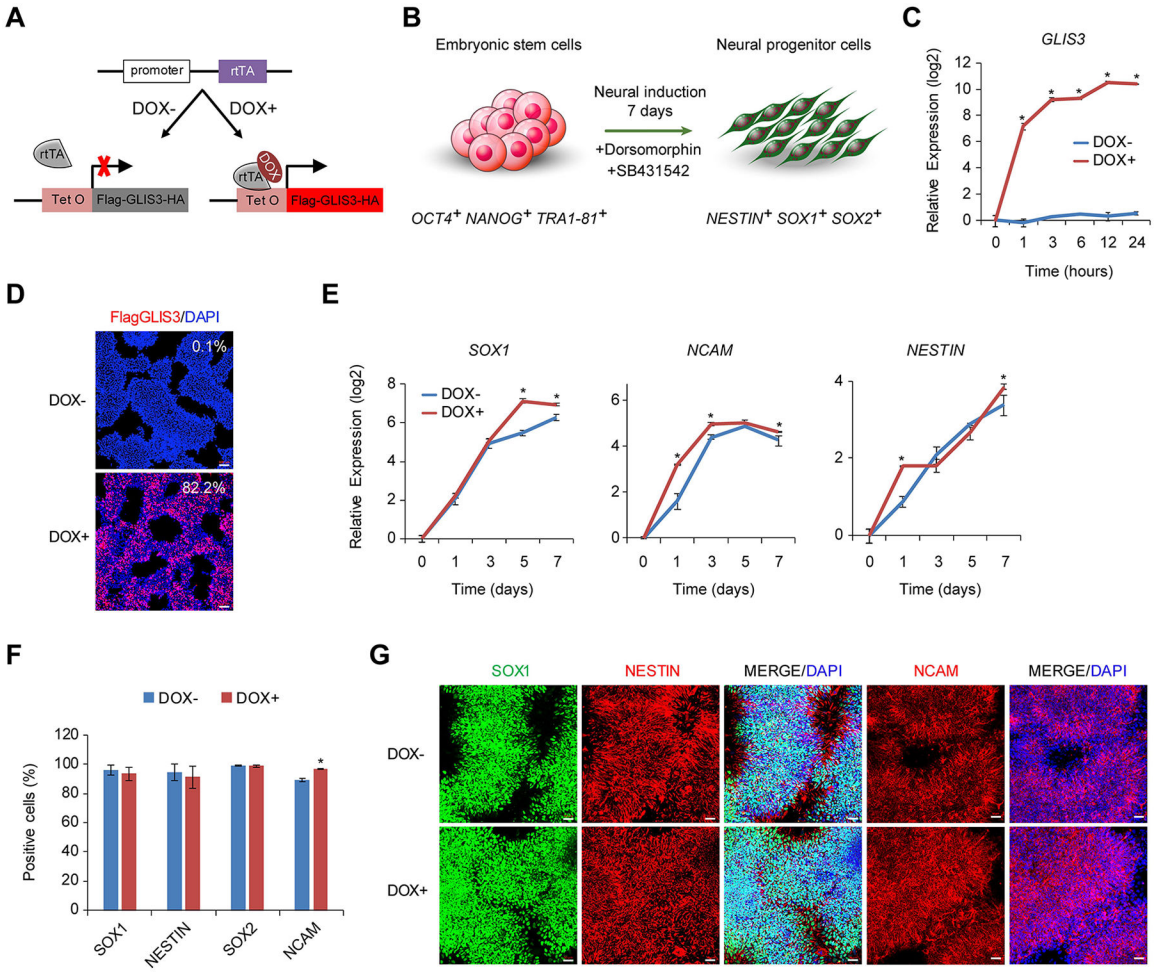

Figure 1. Differentiation of G3-hESC into neural progenitor cells.

(A) Schematic of the pINDUCER20 system encoding Flag-GLIS3-HA under control of a doxycycline (DOX)-inducible promoter used to generate G3-hESCs.

(B) Differentiation protocol using the activin/TGFβ/BMP pathways inhibitors, dorsomorphin and SB431542, to induce differentiation of hESCs into NPCs.

(C) Time course of GLIS3 mRNA induction in G3-hESCs treated with or without DOX as determined by qRT-PCR analysis. Data are normalized to *GAPDH*. Error bars represent SEM of three biological replicates. *p<0.01 (Student's t-test, two-sided).

(D) Representative immunofluorescent images showing induction of Flag-Glis3 protein in G3-hESCs(+) treated for 12 h with or without DOX using anti-Flag M2 antibody. Nuclei are stained by DAPI. The percent Flag-GLIS3$^+$ cells, as determined by FACS analysis, is indicated. Scale bar, 100 μm.

(E) Expression of pan-NPC marker genes, *SOX1*, *NESTIN*, and *NCAM*, during NPC differentiation in G3-hESCs(−) and G3-hESCs(+), as determined using qRT-PCR. Data are normalized to *GAPDH*. Error bars represent SEM of three biological replicates. *p<0.01 (Student's t-test, two-sided).

(F) FACS analysis using antibodies against the pan-neural marker proteins, SOX1, NESTIN, SOX2, and NCAM in G3-NPCs(−) and G3-NPCs(+) at day 7 of NPC differentiation. Error bars represent SEM of three biological replicates. *p<0.01 (Student's t-test, two-sided).
(G) Representative immunofluorescent images showing the expression of pan-neural marker proteins SOX1, NESTIN, and NCAM in G3-NPCs(−) and G3-NPCs(+) at day 7 of NPC differentiation. Scale bar, 50 μm.

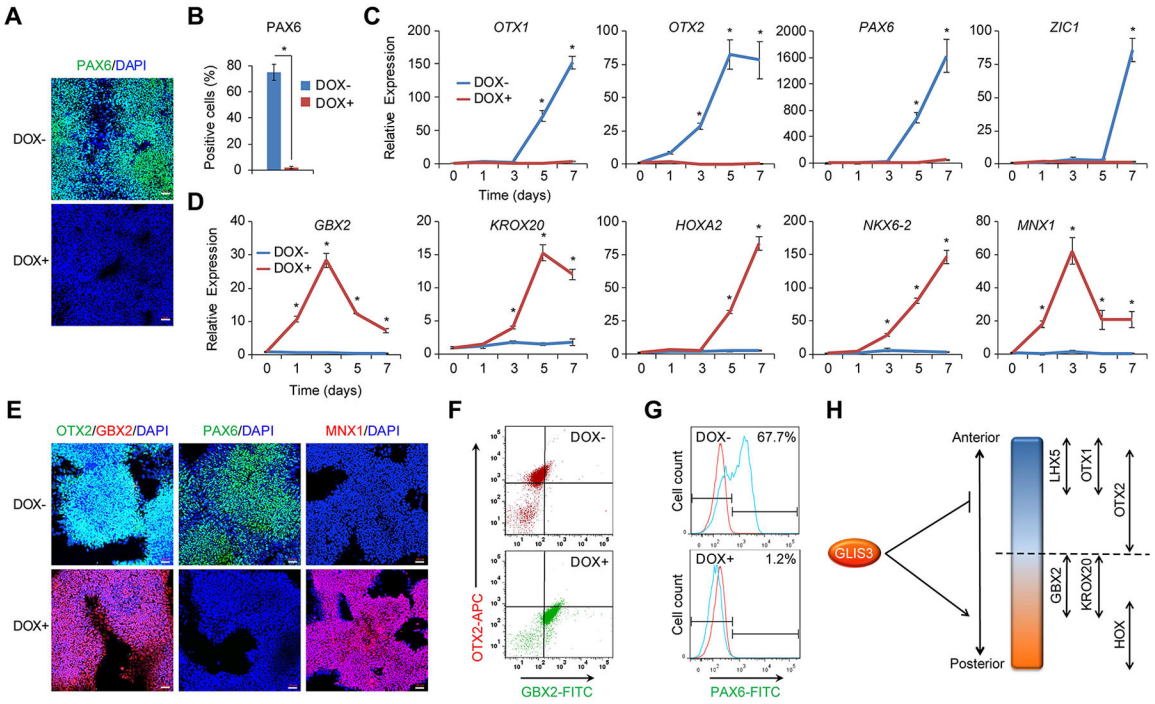

Figure 2. GLIS3 induces a shift in NPC differentiation from the default anterior (A) to the posterior (P) lineage.

(A) Representative immunofluorescent images of NPCs, derived from G3-hESCs treated for 7 days with or without DOX, showing expression of the anterior neural marker PAX6 using a PAX6 antibody. Nuclei were stained with DAPI. Scale bar, 50 μm.

(B) FACS analysis of PAX6+ cells at day 7 of NPC differentiation in G3-hESCs treated with or without DOX. Error bars represent SEM of three biological replicates.

(C) Expression of the anterior marker genes, *OTX1*, *OTX2*, *PAX6*, and *ZIC1* during NPC differentiation of G3-hESCs(−) and G3-hESCs(+), as determined using qRT-PCR. Data are normalized to GAPDH. Error bars represent SEM of three biological replicates. *p<0.05 (Student's t-test, two-sided).

(D) Expression of the posterior marker genes, *GBX2*, *KROX20*, *HOXA2*, *NKX6–2*, and *MNX1* during NPC differentiation of G3-hESCs(−) and G3-hESCs(+), as determined using qRT-PCR. Data are normalized to GAPDH. Error bars represent SEM of three biological replicates. *p<0.05 (Student's t-test, two-sided).

(E) Representative immunofluorescent images of G3-hESCs treated for 5 days with or without DOX showing expression of the anterior marker proteins, OTX2 and PAX6, and posterior markers, GBX2 and MNX1. Nuclei were stained with DAPI. Scale bar, 50 μm.

(F) FACS analysis of G3-hESCs treated for 5 days with or without DOX stained with APC-conjugated anti-OTX2 and FITC-conjugated anti-GBX2 antibodies.

(G) FACS analysis of G3-hESCs treated for 5 days with or without DOX stained with an FITC-conjugated anti-PAX6 antibody.

(F) Schematic view of the expression of key genes involved in A-P patterning of the developing neural tube.

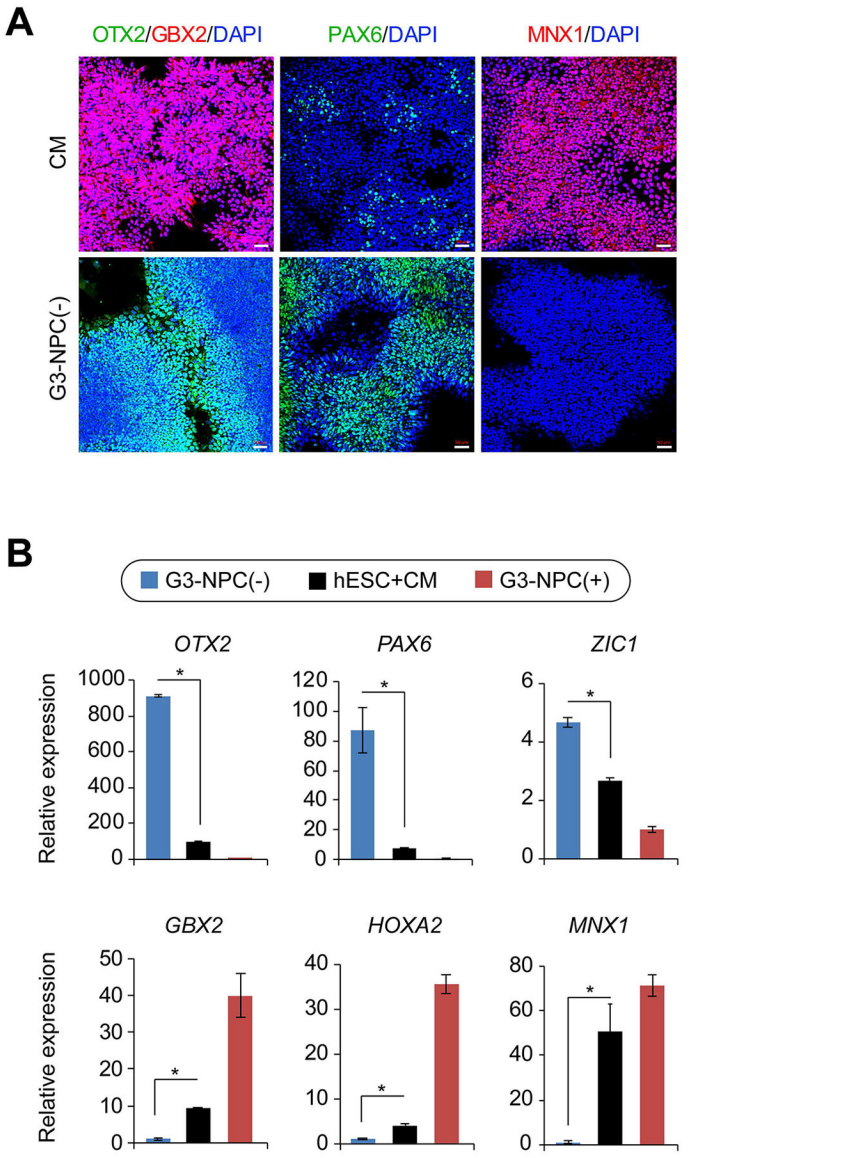

Figure 3. GLIS3-mediated posteriorization in G3-hESC(+) involves paracrine signaling.

(A) Representative immunofluorescent images showing the expression of the anterior marker proteins, OTX2 and PAX6, and posterior markers, GBX2 and MNX1 in parental H9 hESCs, cultured for 5 days in conditioned medium (CM) obtained from G3-NPCs(+) after 24h of DOX treatment, and G3-NPCs at day 5 post-NPC induction without DOX. Nuclei were stained with DAPI. Scale bar, 50 μm.

(B) qRT-PCR analysis of the expression of select A-P marker genes in parental H9 hESCs treated with CM for 5 days compared to that in G3-NPCs at 5 d post-NPC induction with or without DOX. Data are normalized to GAPDH. Error bars represent SEM of three biological replicates. *p<0.01 (One-way ANOVA with Sidak's multiple comparisons test).

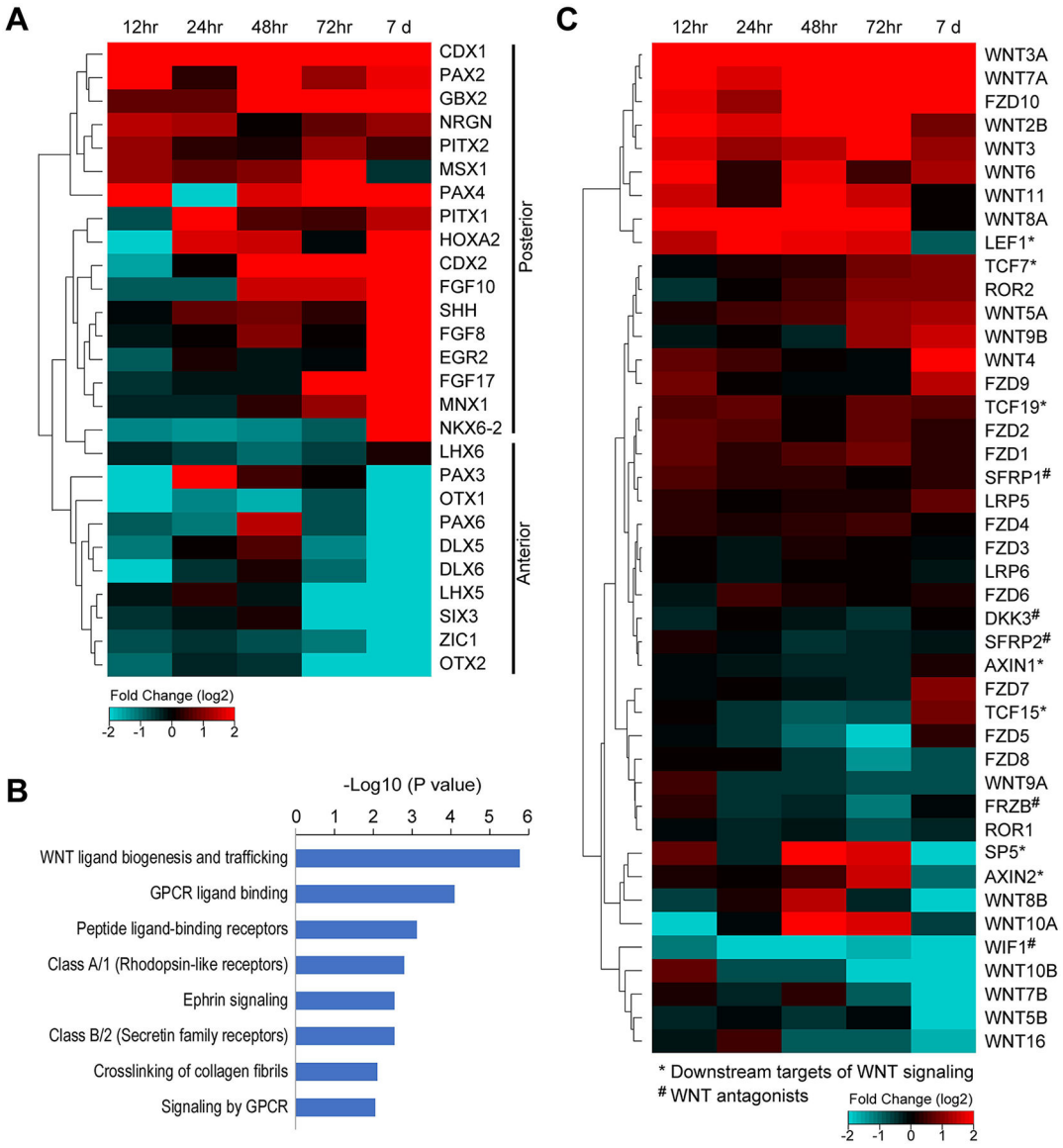

Figure 4. Induction of posterior lineage by GLIS3 is associated with upregulation of several WNT signaling genes.

(A) Heatmap of fold-changes in the expression of A-P patterning genes in G3-hESCs(+) in comparison to G3-hESCs(−) at different times of NPC differentiation. Genes are clustered based on hierarchical clustering of expression changes over time. mRNA expression was analyzed by RNA-Seq.

(B) REACTOME pathway enrichment analyses of genes up-regulated in G3-hESCs(+) at 12 h of NPC differentiation, identifying WNT signaling as a top pathway regulated by GLIS3.

(C) Heatmap of fold-changes in the expression of various WNT signaling-associated genes in G3-hESCs(+) in comparison to G3-hESCs(−) at different times of NPC differentiation.

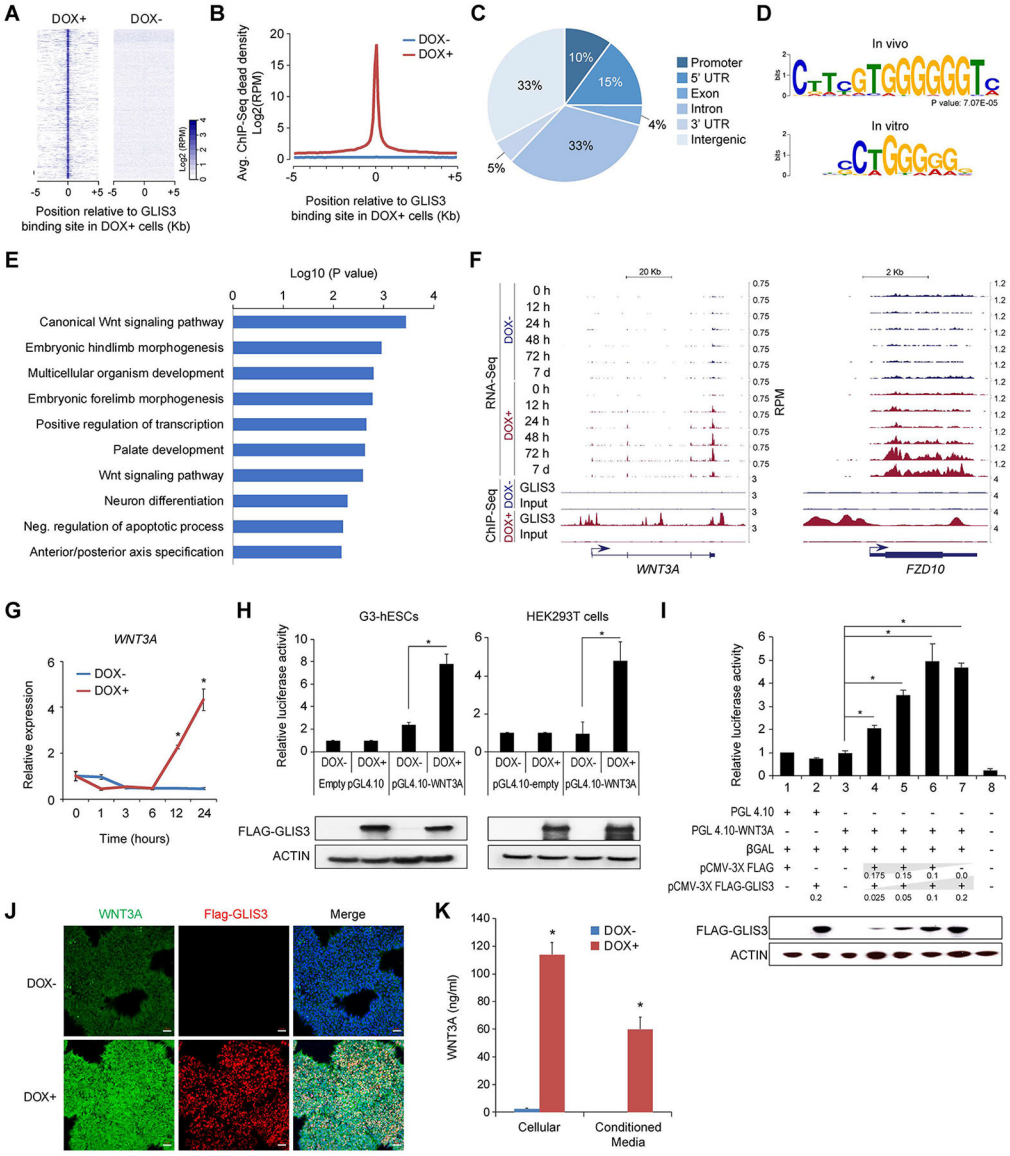

Figure 5. GLIS3 is associated with WNT genes and transcriptionally activates WNT3A.

(A, B) Heatmap (A) and ChIP-Seq read density plot (B) showing GLIS3 occupancy in differentiating G3-hESCs(+) at 12 h of NPC induction.

(C) Genome-wide distribution of the GLIS3 binding sites. Promoter region is defined as the 5 kb region upstream of the transcription start site (TSS).

(D) Consensus sequence motif enriched within *in vivo* GLIS3 binding sites, as determined using *de novo* motif analysis. Also shown is GLIS3 binding sequence previously identified using an *in vitro* binding assay [57].

(E) Gene ontology (GO) enrichment analysis of up-regulated genes targeted by GLIS3 at 12 h of NPC differentiation. Top ten GO categories, with the smallest *P* values, are shown.

(F) Genome browser shots of genes *WNT3A* and *FZD10* showing temporal profiles of gene expression dynamics (RNA-Seq) and GLIS3 occupancy (ChIP-Seq) in G3-hESCs treated

with or without DOX (red and blue tracks, respectively). TSSs and direction of transcription are indicated by arrows.

(G) Temporal profile of *WNT3A* mRNA levels during NPC differentiation of G3-hESCs treated with or without DOX, as determined by qRT-PCR analysis. Data are normalized to *GAPDH*. Error bars represent SEM of three biological replicates. *p<0.01 (Student's t-test, two-sided).

(H) To examine activation of the WNT3A promoter (−1690 to +317 bp relative to TSS) by GLIS3, G3-hESCs and G3-HEK293T cells were transfected with pGL4.10-WNT3A or pGL4.10-empty. *Top*: Relative luciferase activity, in the presence or absence of DOX (24 h). Error bars represent SEM of three biological replicates. *Bottom*: Western blot analysis of Flag-GLIS3 in cells treated with or without DOX. Actin is used as loading control. *p<0.01 (Student's t-test, two-sided).

(I) HEK293T cells were transiently transfected with the pGL4.10-empty or pGL4.10-WNT3A reporter plasmid, pCMV-ß-Gal (transfection control), and different amounts of pCMV-3×Flag-GLIS3 and pCMV-3×Flag as indicated. *Top*: Relative luciferase activity measured 24 h post-transfection. Error bars represent SEM of three biological replicates. *Bottom*: Western blot analysis of Flag-GLIS3. Actin is used as loading control. *p<0.01 (One-way ANOVA with Sidak's multiple comparisons test).

(J) Representative immunofluorescent images showing the expression of WNT3A and Flag-GLIS3 in differentiating G3-hESCs(−) and G3-hESCs(+) at 24 h of post-NPC induction, using anti-WNT3A and anti-Flag M2 antibodies, respectively. Nuclei were stained by DAPI. Scale bar, 50 mm.

(K) Relative levels of cellular or secreted (conditioned medium) WNT3A protein in G3-hESCs(−) and G3-hESCs(+) at 24 h of NPC induction. Error bars represent SEM of three biological replicates. *p<0.01 (Student's t-test, two-sided).

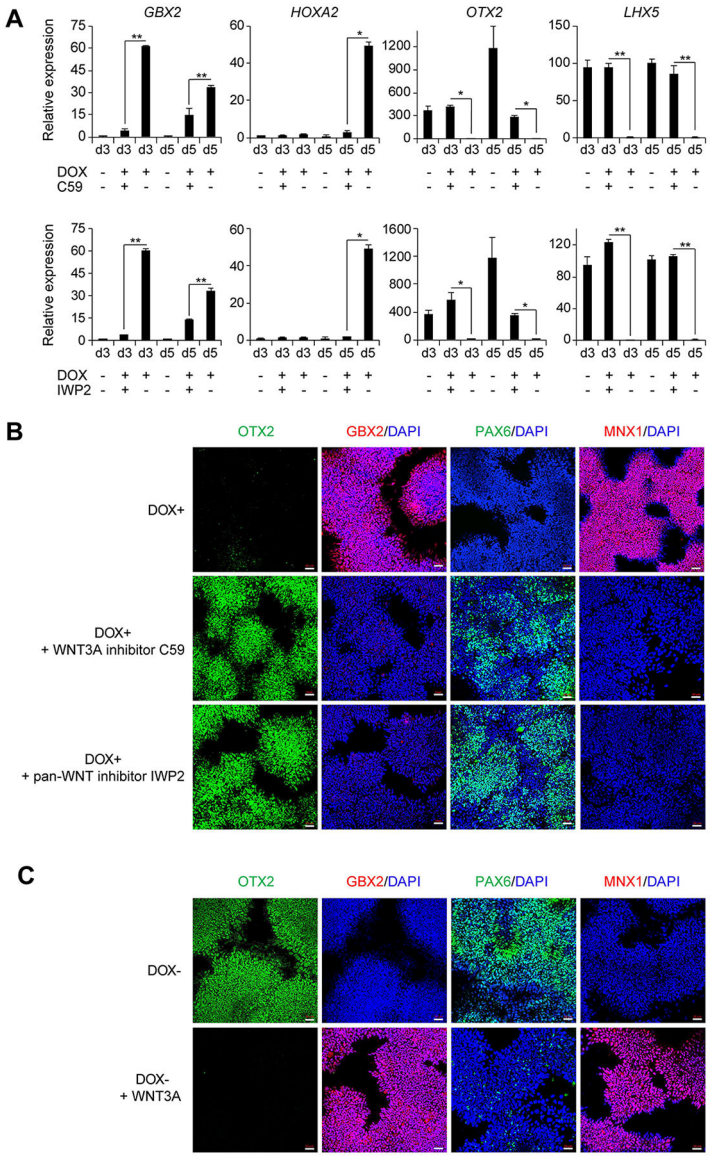

Figure 6. GLIS3-mediated posterior patterning is WNT-dependent.

(A) Inhibition of GLIS3-induced posterior NPC differentiation in G3-hESCs(+) cells by WNT inhibitors, WNT-C59 (top) or IWP2 (bottom). G3-hESCs were treated with and without DOX and in the presence or absence of 100 nM WNT-C59 (top) or 2 μM IWP2 for 3 or 5 days as indicated. Cells were then analyzed by qRT-PCR for their expression of several A-P-related genes. Data are normalized to *GAPDH*. Error bars represent SEM of three biological replicates. *p<0.05, **p<0.01 (Two-way ANOVA with Sidak's multiple comparisons test).

(B) Representative immunofluorescent images showing the expression of anterior protein markers, OTX2 and PAX6, and posterior markers, GBX2 and MNX1, at day 3 post-NPC induction in the presence of DOX with or WNT inhibitors C59/IWP2. Nuclei were counterstained by DAPI. Scale bar, 50 μm.

(C) Representative immunofluorescent images showing the expression of anterior protein markers, OTX2 and PAX6, and posterior markers, GBX2 and MNX1, in G3-hESCs(−) treated with recombinant WNT3A (200 ng/ml) for 3 days. Nuclei were counterstained by DAPI. Scale bar, 50 μm.

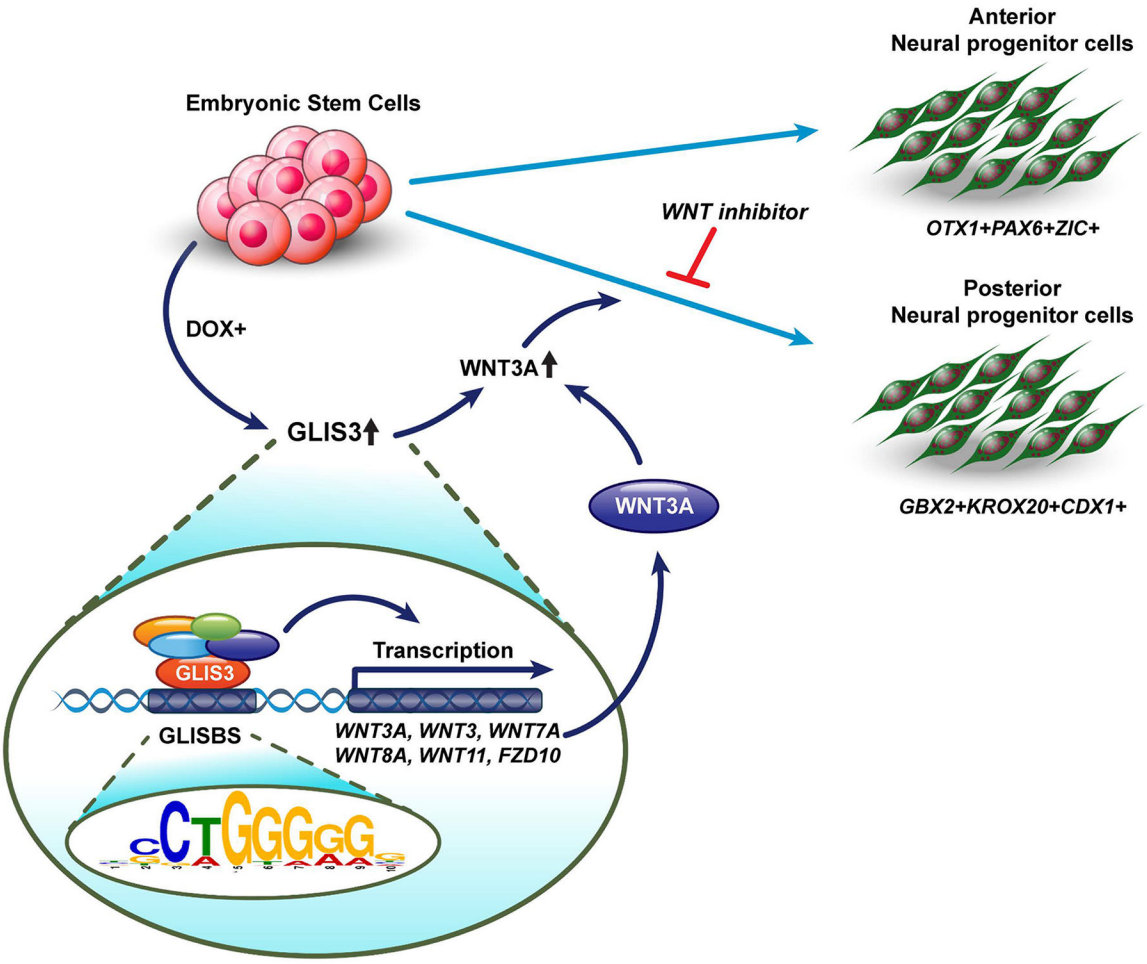

Figure 7. Proposed model for GLIS3-mediated shift in neural progenitor cell lineage specification.

GLIS3 directly activates the transcription of *WNT3A* and other WNT-related genes causing increased synthesis and secretion of the strong posteriorizing factor, *WNT3A*, and other WNT proteins inducing a shift from the default anterior to the posterior neural lineage. The strong inhibition of GLIS3-induced posteriorization by WNT inhibitors and the efficient induction of posteriorization by G3-hESCs(+) conditioned medium supports the conclusion that activation of WNT signaling is a major mediator of GLIS3-induced posterior specification.